Eleventh U.S. National Conference on Earthquake Engineering
Integrating Science, Engineering & Policy
June 25-29, 2018
Los Angeles, California

SYSTEM IDENTIFICATION OF A MID-RISE COLD-FORMED STEEL FRAMED BUILDING UNDER EARTHQUAKE AND POST-EARTHQUAKE FIRE TESTS

X. Wang[1] and T.C. Hutchinson[2]

ABSTRACT

Cold-formed steel has many natural benefits to offer when utilized as the primary load resisting system in buildings. Amongst them, its high strength to weight ratio and inherent non-combustibility result in a material with the promise to offer resiliency following both earthquake and post-earthquake fire hazard scenarios. However, the evolution of buildings dynamic characteristics considering such a multi-hazard loading scenario (earthquake and ensuing fire demands) has thus far observed little attention in the literature. This is largely due to a paucity of data in this regard. Using the experimental data collected from a recently performed full-scale shake table test of a mid-rise cold-formed steel (CFS) building, various system identification methods are utilized to monitor the evolution of dynamic properties of the test building. This building was subjected to a unique multi-hazard scenario including earthquake, post-earthquake fire, and finally post-fire earthquake loading with companion low-amplitude vibration tests, including ambient vibrations and white noise base excitation tests, throughout the construction and the test phase. This paper presents a comprehensive system identification study to understand the evolution of the modal parameters (i.e., natural frequencies, damping ratios, and mode shapes) of the building throughout the test program. The modal parameters of the building are estimated using time-domain system identification techniques. Agreement between the evolution of the modal parameters and the progression of physical damage demonstrates the effectiveness of the system identification techniques for structural damage assessment.

[1]Post-doctoral Researcher, Dept. of Structural Engineering, University of California, San Diego, La Jolla, CA 92093
[2]Professor, Dept. of Structural Engineering, University of California, San Diego, La Jolla, CA 92093 (email: tara@ucsd.edu)

Wang X, Hutchinson T.C. System identification of a mid-rise cold-formed steel framed building under earthquake and post-earthquake fire tests. *Proceedings of the 11th National Conference in Earthquake Engineering*, Earthquake Engineering Research Institute, Los Angeles, CA. 2018.

System identification of a mid-rise cold-formed steel framed building under earthquake and post-earthquake fire tests

X. Wang[1] and T.C. Hutchinson[2]

ABSTRACT

Cold-formed steel has many natural benefits to offer when utilized as the primary load resisting system in buildings. Amongst them, its high strength to weight ratio and inherent non-combustibility result in a material with the promise to offer resiliency following both earthquake and post-earthquake fire hazard scenarios. However, the evolution of buildings dynamic characteristics considering such a multi-hazard loading scenario (earthquake and ensuing fire demands) has thus far observed little attention in the literature. This is largely due to a paucity of data in this regard. Using the experimental data collected from a recently performed full-scale shake table test of a mid-rise cold-formed steel (CFS) building, various system identification methods are utilized to monitor the evolution of dynamic properties of the test building. This building was subjected to a unique multi-hazard scenario including earthquake, post-earthquake fire, and finally post-fire earthquake loading with companion low-amplitude vibration tests, including ambient vibrations and white noise base excitation tests, throughout the construction and the test phase. This paper presents a comprehensive system identification study to understand the evolution of the modal parameters (i.e., natural frequencies, damping ratios, and mode shapes) of the building throughout the test program. The modal parameters of the building are estimated using time-domain system identification techniques. Agreement between the evolution of the modal parameters and the progression of physical damage demonstrates the effectiveness of the system identification techniques for structural damage assessment.

Introduction

In recent decades, structural health monitoring has attracted significant attention amongst civil engineers as it offers the prospect of assessing the condition and detecting potential damage of structures under extreme events (e.g., earthquakes, hurricanes) or long-term effects (e.g., corrosion) [1]. As one of the most widely used non-destructive damage detection techniques, system identification relies on changes in the identified modal parameters (i.e., natural frequencies, damping ratios, and mode shapes) or quantities subsequently derived to detect and localized potential damage of a structure under a routine maintenance plan or following a hazard event, since these parameters are correlated with the change of physical characteristics of the structure (e.g., mass, stiffness, and energy dissipation mechanisms). The modal parameters are often identified from low-amplitude vibration data recorded on the real structures, which are considered as equivalent linear viscously-damped dynamic systems in the identification procedures. Depending

[1]Post-doctoral Researcher, Dept. of Structural Engineering, University of California, San Diego, La Jolla, CA 92093
[2]Professor, Dept. of Structural Engineering, University of California, San Diego, La Jolla, CA 92093 (email: tara@ucsd.edu)

Wang X, Hutchinson T.C. System identification of a mid-rise cold-formed steel framed building under earthquake and post-earthquake fire tests. *Proceedings of the 11th National Conference in Earthquake Engineering*, Earthquake Engineering Research Institute, Los Angeles, CA. 2018.

on the availability of input excitation sources, experimental (input-output) and operational (output-only) modal analysis procedures are the main methods used for extracting the modal parameters from recorded vibration data. Interested readers are referred to [2,3] for a comprehensive overview of vibration-based system identification techniques.

This paper investigates the modal characteristics of a full-scale six-story CFS framed building under earthquake and post-earthquake fire test program [4-6]. Within a three-week test program, the CFS test building was subjected to seven earthquake tests of increasing motion intensity before and two earthquake tests after the live fire tests at select locations of the building. Complementing the earthquake and fire test sequence, low-amplitude vibration tests were conducted throughout the construction and testing phases to allow for identification of the dynamic characteristics of the building. This paper systematically studies the evolution modal parameters of the building identified from the white noise (WN) base excitation tests during the test phase. The identified modal characteristics of the building provide quantified metrics that correlate well with the progression of the building physical damage throughout the test program.

Test Building

The six-story CFS framed test building was assumed to be located in a high seismic region near downtown Los Angeles, with its design basis complying with current code provisions [7-9]. With a uniform plan dimension of 10.4 m × 7.3 m at each floor, the test specimen occupied almost the entire 12.2 m × 7.6 m shake table footprint (Fig. 1). The total height of the building was 19.2 m above the shake table platen (with a floor-to-floor height of 3.1 m for all stories and a 1.2 m-tall parapet on the roof perimeter). The primary lateral load resisting system in the direction of shaking (longitudinal axis of the building) consisted of two longitudinal shear walls placed along the corridor, while the corner shear walls were assumed to resist transverse and torsion loads (Fig. 1b). It is noted that, except for the first-story wall system that was fabricated in-situ, the structural skeleton of the building was constructed using prefabricated wall and floor panels, which significantly expedited the construction process. Additional details regarding the building design and the structural systems are available in [4-6].

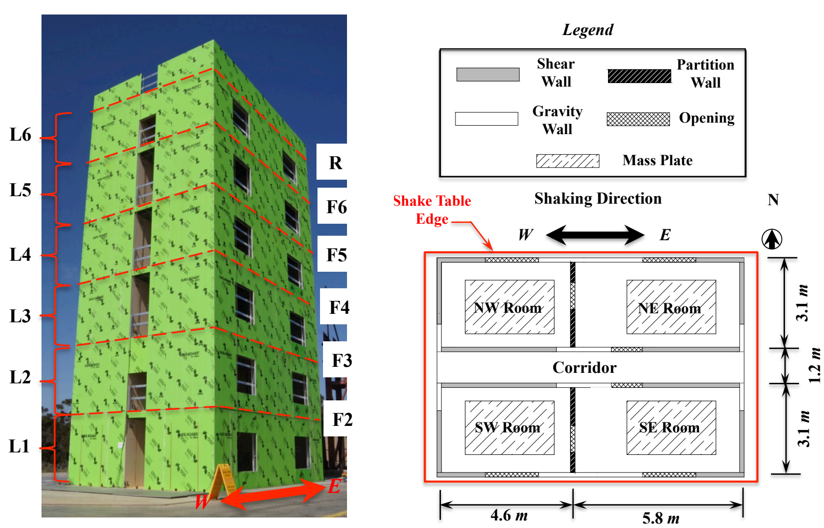

(a) (b)

Figure 1. Test building: (a) isometric photograph, and (b) schematic building plan layout (typical of floor 2 to 6).

Earthquake and Fire Tests

The three-week test program consisted of a sequence of nine earthquake tests and six fire tests between June 13 and July 1, 2016. In three test days of the pre-fire test phase (June 13, 15, and 17, 2016), the building was subjected to seven earthquakes with increasing motion intensity levels, namely, serviceability, design, and maximum considered earthquake (MCE) events. Subsequently, live fire tests were conducted on the earthquake-damaged building at two select levels (level 2 and 6) of the building across a period of three consecutive days (June 27–29, 2016). The test program concluded with two post-fire earthquake tests (serviceability followed by MCE events) on the final test day (July 1, 2016). The earthquake-fire test sequence as well as the peak building responses associated with individual earthquake tests are summarized in Table 1. It is noted that the seismic drift demands, such as peak intersotry drift ratio (PIDRs) and peak roof drift ratios (PRDRs), serve as important proxies for assessing the structural damage of the test building.

Table 1. Summary of the test sequence and the associated peak building responses

Earthquake Test Date	*Test Motion*	*Performance Target*	*PFA (g) (Floor #)*	*PIDR (%) (Level #)*	*PRDR (%)*	*RDR_{res} (%)*
Day 1 (June 13, 2016)	EQ1:RIO-25	Serviceability	0.35 (R)	0.08 (L4)	0.05	0.0
	EQ2:CNP-25		0.38 (R)	0.09 (L4)	0.07	0.0
	EQ3:CUR-25		0.45 (R)	0.10 (L4)	0.08	0.0
Day 2 (June 15, 2016)	EQ4:CNP-25		0.43 (R)	0.10 (L4)	0.09	0.0
	EQ5:CNP-50	50% Design	0.85 (R)	0.24 (L3)	0.19	0.0
	EQ6:CNP-100	Design	2.07 (R)	0.89 (L4)	0.70	0.0
Day 3 (June 17, 2016)	EQ7:CNP-150	MCE	3.77 (F5)	1.70 (L4)	1.49	0.1
Fire Test Sequence (June 27–29, 2016)						
Day 4 (July 1, 2016)	EQ8:RIO-25	Serviceability	0.16 (R)	0.17 (L3)	0.12	0.0
	EQ9:RRS-150	MCE	4.43 (F5)	12.15 (L2)	2.84	1.2

Notes: PFA – peak floor acceleration; PIDR – peak interstory drift ratio; PRDR – peak roof drift ratio; RDR_{res} –residual roof drift ratio; MCE – maximum considered earthquake.

Fig. 2 shows the typical physical damage of the test building throughout the test phase. The physical damage was documented at distinct inspection stages following the completion of all earthquake tests within individual test days. Qualitatively, one can observe damage ranging in severity from minor, moderate, to severe. Due to the low seismic drift demands (PIDR < 0.1%) during the serviceability level test sequence (EQ1–EQ4) at all levels of the test building, the test building sustained only a few instances of minor damage in the form of localized gypsum crushing or bulging (Fig. 2a) and incipient screw withdrawal (Fig. 2b) at level 3 and 4. Damage to the interior sheathing continued to develop as the drift demand increased progressively during the last three pre-fire earthquake tests (PIDR attained ~1% during EQ6 and exceeded 1.5% during EQ7). Screw withdrawal and gypsum crushing of the shear walls and gravity walls became more pervasive at all levels (Fig. 2c-d). Following the completion of the pre-fire earthquake test sequence, inspection of the framing studs and tracks of select shear walls at level 4 (the level with the largest drift demands) revealed no apparent damage to the wall framing of the wall systems. Due to the extremely large drift demands of the test building (PIDR > 12% at level 2 and residual

RDR > 1%), the building developed a soft-story mechanism at the completion of the post-fire extreme earthquake event (EQ9), resulting in extremely severe damage to the wall systems at level 2 (Fig. 2e). However, the test building resisted collapse despite the excessive drift demands. Additional details regarding the building response and physical damage are available in [5].

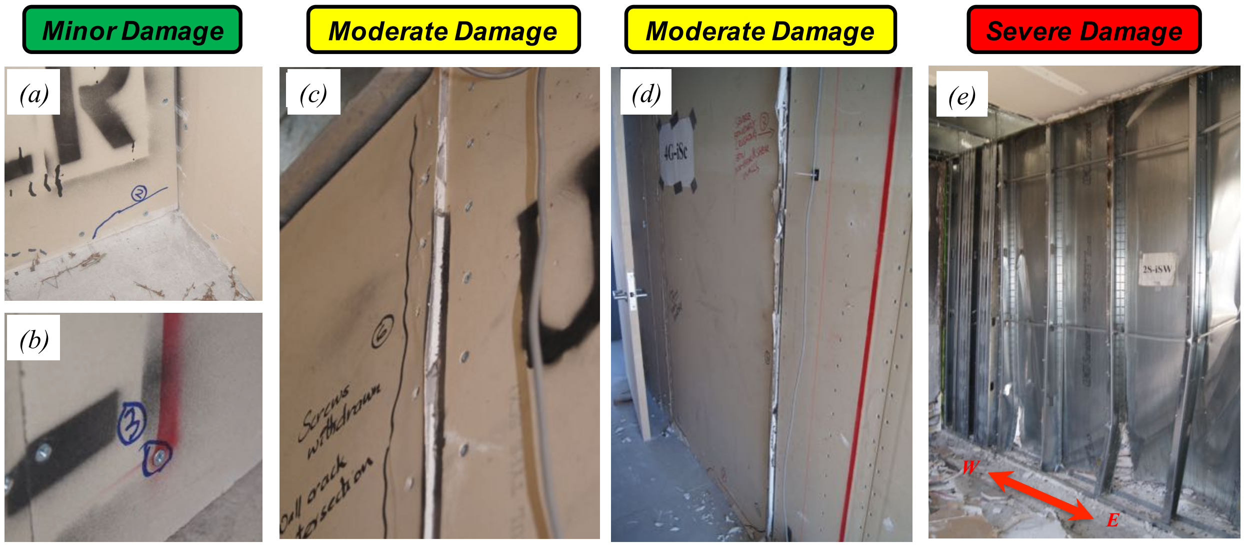

Figure 2. Physical damage of CFS wall systems: (a) gypsum corner crushing (after EQ3), (b) incipient screw withdrawal (after EQ3), (c) wall boundary crushing (after EQ6), (d) wall boundary crushing (after EQ7), and (e) buckled framing studs following detachment of gypsum panels (after EQ9).

System Identification

Low-amplitude Vibration Tests

To allow for identification of the building dynamic characteristics, a sequence of low-amplitude vibration tests, including 22 WN tests and 4 ambient vibration tests, was performed throughout the earthquake-fire test phase. Fig. 3 shows the timeline of the low-amplitude vibration test sequence throughout the test phase as well as a total of eleven states (S0–S10) across the timeline. Each state represents a specific damage condition for the test building. While the ambient vibration tests occurred only at the beginning and end of the pre-fire and post-fire test phases, the WN tests were consistently conducted before and after each earthquake test except at the end the test program (state S10) due to the severity of damage to the test building.

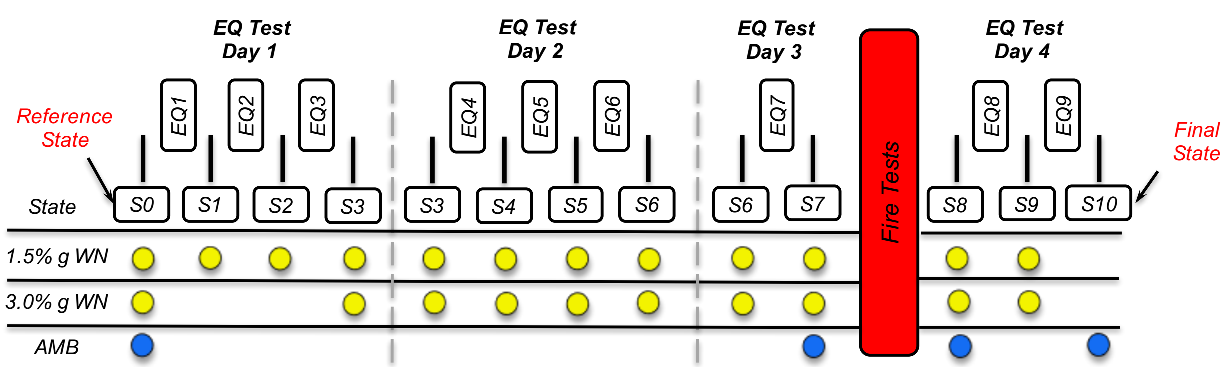

Figure 3. Timeline of low-amplitude vibration test sequence throughout the test phase.

Each of the WN tests was about 180 seconds (3 minutes) in duration. The amplitude of the WN tests, as quantified by the root-mean-square (RMS) acceleration of the input excitation, was either 1.5% g or 3.0% g (hereafter referred to as 1.5% g or 3.0% g WN test). The accelerations of the test building and the shake table platen were measured using an array of uniaxial MEMS accelerometers sampling data at a frequency of 240 Hz. Fig. 4 shows the sample acceleration histories measured at the table platen and the roof during the 1.5% g WN at state S0 (reference state). Since the white noise excitation was applied along the longitudinal axis of the building using the single-axis shake table, the amplitudes of the transverse accelerations (both table platen and roof) were substantially smaller (about 5%) than their longitudinal counterparts. The non-comparable amplitudes of the excitations resulted in much lower modal participation of the transverse modes and smaller signal-to-noise ratio for the transverse building response, which lead to difficulties for transverse mode identification as discussed in the following section.

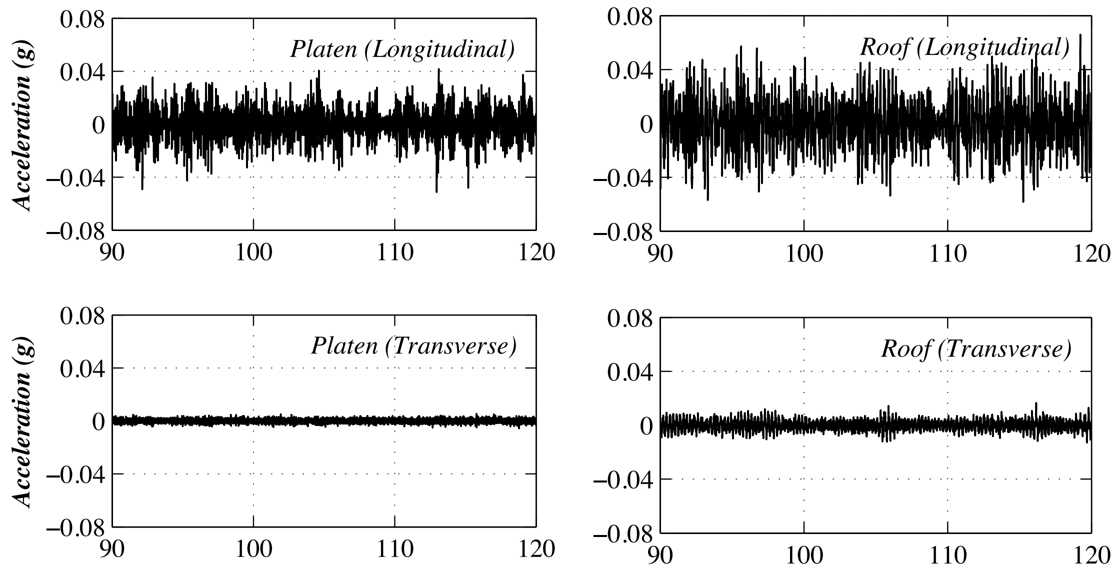

Figure 4. Table platen and building roof accelerations measured during the 1.5% g WN test at state S0 (reference state).

Method and Validation

Depending on the availability of input excitation sources, identification the modal parameters (natural frequencies, damping ratios, and mode shapes) of a structure can be classified into either input-output or output-only methods. Due to the length restrictions, this study focuses on presenting the modal parameters of the test building extracted using the deterministic-stochastic identification (DSI) method [10], which is a time-domain system identification method that realizes a linear state-space model using input-output data. This method has been successfully implemented to identify the modal parameters of the large-scale structures in previous shake table tests [11–13].

In the DSI method, the system input to the test building is taken as the averaged longitudinal acceleration measured at the table platen, whereas the system output involves longitudinal floor accelerations (measured at the northwest and southwest corners) and transverse floor accelerations (measured at northwest and northeast) at each floor from the second floor to the roof (a total of 24 output channels). In the data pre-processing, the measured raw acceleration histories are first decimated to 120 Hz to reduce the computational costs and subsequently filtered using a 4th order band-pass Butterworth filter (with cut-off frequencies at 0.25 Hz and 25 Hz). It is noted that the Nyquist frequency of the processed data of 60 Hz remains sufficiently large to involve all the vibration modes that contribute noticeably to the building response. To distinguish structural modes from spurious (mathematical) modes in the system identification procedures, stability diagrams are employed to examine the consistency of identified modal parameters over a consecutive sequence of model orders [14]. In this study, the stability thresholds of the identified modal parameters is taken as a relative error of 0.02, 0.05, and 0.05 for frequency, damping ratio, and modal assurance criterion (MAC) [15], respectively. The identified mode is considered as stable when the triple convergence criteria (frequency, damping, and mode shape) are satisfied for at least six consecutive model orders.

According to the convergence criteria as mentioned above, a total of six stable modes are identified using the DSI method. Fig. 5 illustrates the mode shapes of the stable modes and the corresponding polar plot representations of the complex-valued mode shapes at state S0 (reference state). Absent substantial stiffness and mass irregularities for the test building, the first three identified modes correspond to the first transverse (1-T), longitudinal (1-L), and torsional (1-To) vibration modes, whereas the last three identified modes correspond to the second transverse (2-T), longitudinal (2-L), and torsional (2-To) vibration modes. In addition, the polar plots indicate that all the identified modes are nearly classically damped because the mode shape components are nearly collinear. It is noted, however, that the convergence thresholds are more difficult to be achieved by the transverse modes, since the small amplitude of the transverse response tends to result in less stable modal parameters (particularly the damping ratios) across different model orders.

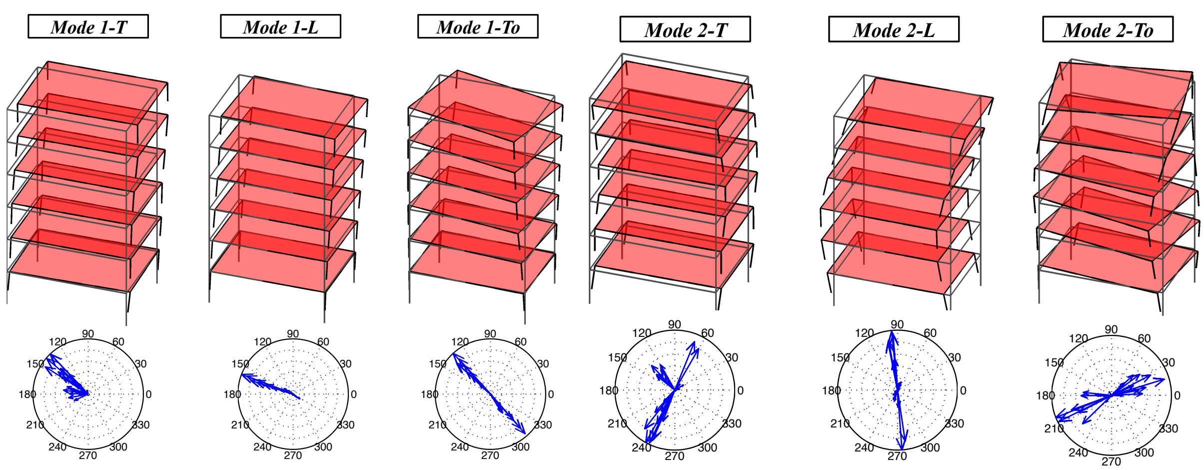

Figure 5. Mode shapes and the corresponding polar plot representation of the mode shape vectors (1.5% g WN test at state S0 – reference state).

For the purpose of validating the DSI method, Fig. 6 compares the measured longitudinal floor accelerations of three select floors (floor 2, floor 4, and roof) with the corresponding responses predicted using the identified state-space model during the 1.5% g WN tests at the beginning and the end of the pre-fire test sequence (states S0 and S7). Agreement between the measured and predicted responses demonstrates the effectiveness of the identified model in replicating the dynamic responses of the building during the WN tests. However, discrepancies between the measured and predicted response increase as the building damage progressed as a result of increased nonlinearity due to damage progression. It is also observed that the measured floor accelerations at state S7 became apparently smaller than their counterparts at state S0 as a result of damage-induced building period elongation as a result of structural damage accumulated throughout the pre-fire earthquake test sequence (EQ1–EQ7).

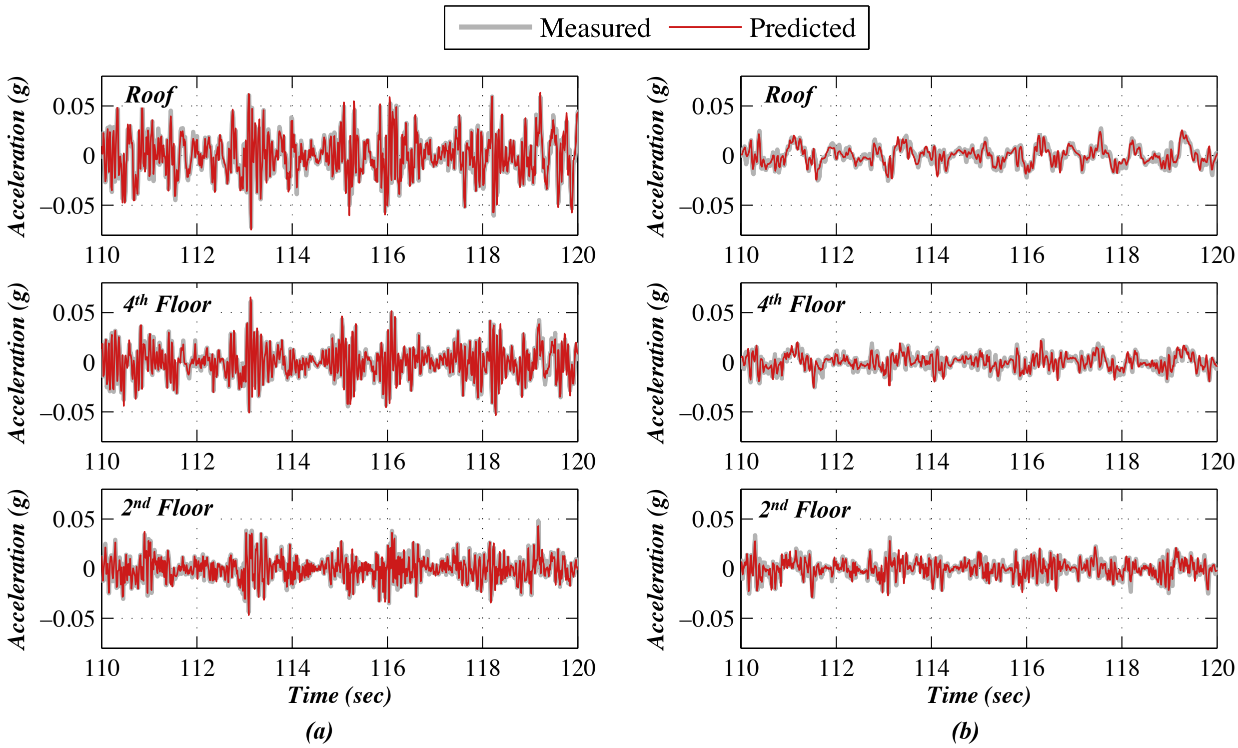

Figure 6. Comparison of measured and predicted longitudinal floor accelerations during 1.5% g WN tests: (a) state S0 (reference state), and (b) state S7 (end of pre-fire test sequence).

Modal Parameters Evolution

Using the WN test data recorded at a total of 10 stages during the test phase (state S0–S9), the modal parameters of the test building are identified using the DSI method. Fig. 7 shows the identified natural frequencies (left column) and the damping ratios (left column) of the longitudinal (1-L and 2-L) and torsional (1-To and 2-To) vibration modes. The transverse vibration modes are not shown due to the convergence difficulties resulted from the non-comparable amplitudes of the response between the longitudinal and transverse directions. It is also noted that the modal parameters of the two higher modes (2-L and 2-To) are identified only from the 1.5% g WN test data at state S6–S9, since the building suffered substantial damage following the design event test EQ6.

As clearly indicated in Fig. 7, damage progression of the test building leads to decrease of the natural frequencies but increase of damping ratios for all the identified vibration modes. While varying only slightly between state S0 and S4 (service level test sequence), the identified natural frequencies dropped significantly at state S6 (following the design event EQ6) when the damage to the building wall systems became pervasive (Fig. 2c). In contrast, the identified damping ratios increased sharply at state S5 and S6 as a result of the damage accumulation at the earthquake events EQ5 and EQ6. The identified modal parameters are also found to be dependent on the amplitude of the WN excitations. The increase of the excitation amplitude (from 1.5% g to 3.0% g) consistently reduces the natural frequencies and increases the damping ratios at each of the ten states (S0–S10). In addition, the damping ratios of the higher modes (2-L and 2-To) appear smaller compared to those of their respective fundamental modes (1-L and 1-To). During the serviceability level test sequence (S0–S4), the identified damping ratio larger than 5% for the first longitudinal mode (1-L) but only about 3% for the second longitudinal mode (2-L) This is likely due to the greater hysteretic energy dissipation associated with the fundamental modes as a result of its large modal contribution, which is idealized as equivalent viscous damping in the identification method.

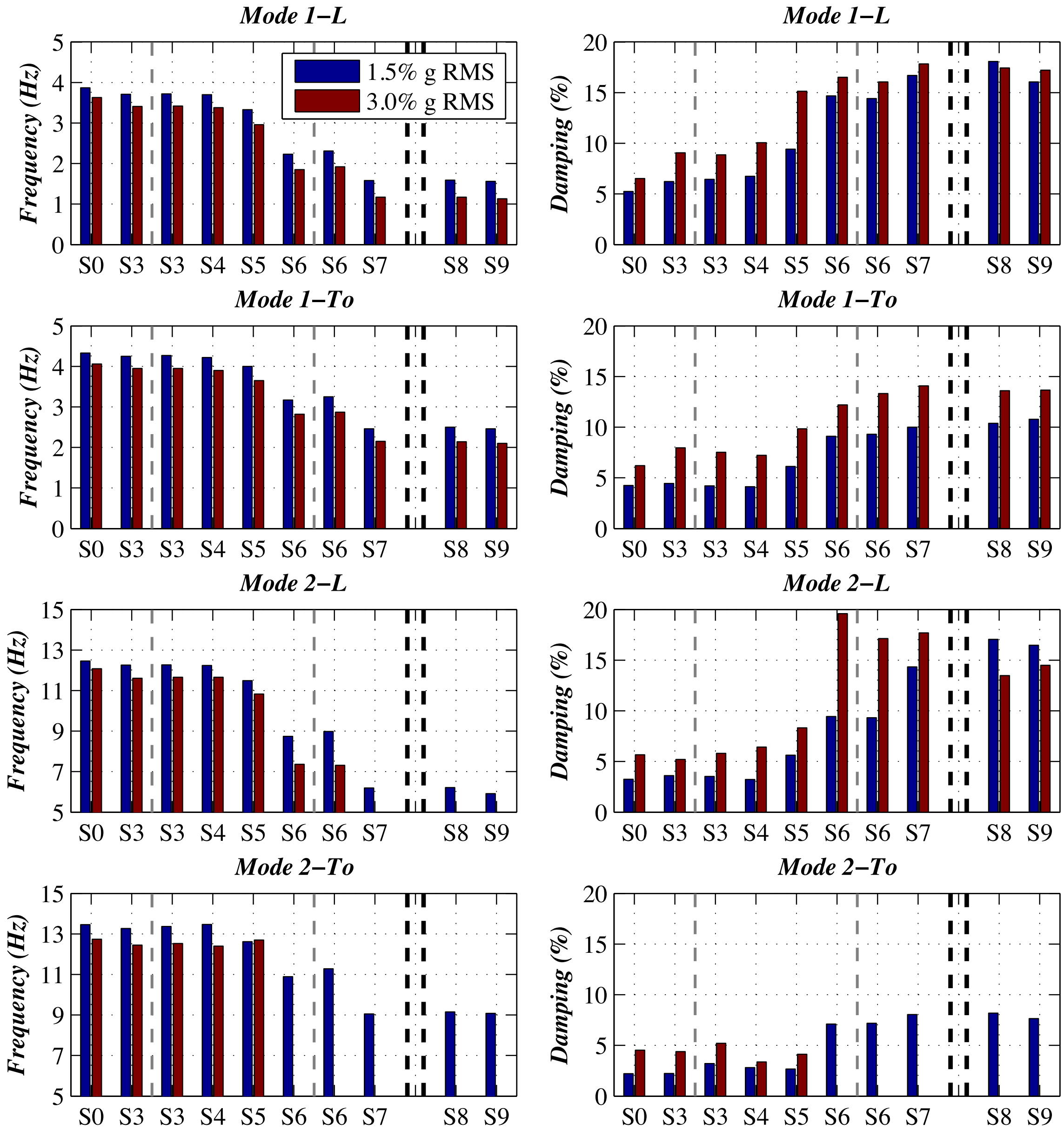

Figure 7. Natural frequencies and damping ratios of the test building identified from the WN tests (single dashed line – test day divider, double dashed line – fire test phase).

Fig. 8 shows the frequency losses of the first longitudinal and torsional vibration modes mode (1-L and 1-To) during the test phase. The overall frequency loss trends of the two vibration modes both correlate well with the building damage progression throughout the test program. As physical damage occurred only in the form of local gypsum crushing and incipient screw withdrawal (Fig. 2a-b) during the serviceability level earthquake test sequence (EQ1–EQ4), the frequency loss remained sufficiently small (< 10%) at this stage. As damage of the test building sustained more pervasive damage (Fig. 2c-d) following the design event EQ6 and MCE event EQ7, the frequency losses achieved 40% at state S6 and exceeded 50% at S7. No further loss of the frequencies occurred following the fire tests (state S8) and the post-fire serviceability level event EQ8, although the fire tests at level 2 and 6 resulted in considerable damage to the gypsum sheathing induced by elevated temperature. This is explained by the fact that the earthquake-induced damage accumulated during the pre-fire test phase (EQ1–EQ7) outweighed the effect of fire-induced damage.

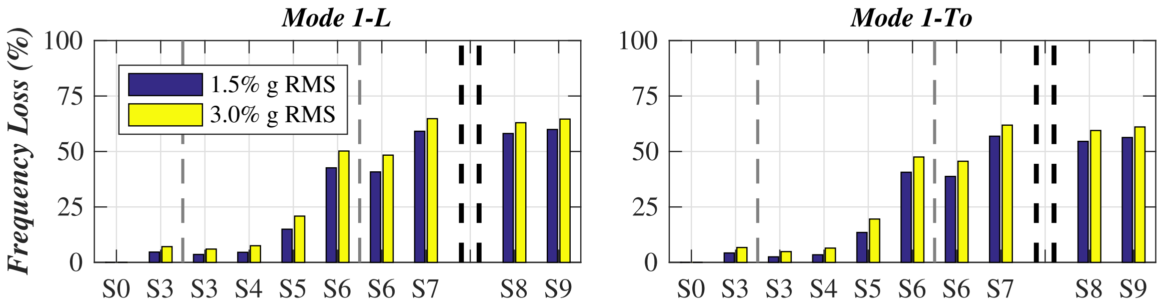

Figure 8. Frequency losses of the first longitudinal and first torsional modes (single dashed line – test day divider, double dashed line – fire test phase).

Conclusions

Understanding the evolution of the dynamic characteristics of a building considering a multi-hazard loading scenario (earthquake and ensuing fire demands) has, to the authors' knowledge, thus far not been studied in the literature. This is largely due to a paucity of data available to support such analysis. Using low-amplitude vibration data collected from a recently performed earthquake and post-earthquake tests of a full-scale mid-rise cold-formed steel (CFS) building, various system identification methods are utilized to track the evolution of dynamic properties (i.e. modal frequencies, damping, mode shapes) of the system under a unique multi-hazard loading scenario. In particular, the test building was subjected to a multi-hazard scenario including earthquake, post-earthquake fire, and finally post-fire earthquake loading with companion low-amplitude vibration tests, including ambient vibrations and white noise base excitation tests, throughout the construction and the test phase. Test data recorded from the low-amplitude vibration tests allow for systematic study of the evolution of the modal parameters. Key findings from the system identification study are summarized as follows:

- Damage progression of the test building resulted in reduced natural frequencies and increased damping ratios. The frequency losses remained sufficiently small (< 10%) during the serviceability level earthquake test sequence but increased substantially following the design level test (achieved 40%) and the MCE level test (exceeded 50%) due to much larger seismic drift demands. However, the fire tests induced no further frequency losses. The evolution of these modal parameters correlates well with the progression of structural damage during the earthquake and fire tests, demonstrating the effectiveness of the vibration-base identification method for monitoring structural health.
- The natural frequencies and damping ratios are dependent on the amplitude of the WN input excitation. Increasing the amplitude of the input excitation tends to reduce the natural frequency but increase the damping ratios. This is a well-known disadvantage of the use of low

amplitude vibration in the context of system identification.

- The damping ratios of the higher modes appear slightly smaller than those of their respective fundamental modes. This is likely due to the larger hysteretic energy dissipation related to the fundamental modes as a result of its large modal contribution.

Acknowledgments

This research project is a collaboration between two academic institutions (University of California, San Diego and Worcester Polytechnic Institute), two government or institutional granting agencies (Department of Housing and Urban Development and the California Seismic Safety Commission) and 15 industry partners. We also thank the Jacobs School of Engineering and Department of Structural Engineering at UCSD for matching support of this effort. Specific industry individuals that dedicated significant time included Fernando Sesma, Kelly Holcomb, Carleton Elliot and Tyler Elliot, Harry Jones, Diego Rivera, Doug Antuma, Larry Stevig, Tim Reinhold and Warner Chang, Steve Helland, Rick Calhoun, and Jesse Karnes. We appreciate the efforts of these individuals and their colleagues at their respective firms. Regarding support for the test program, the efforts of NHERI@UCSD staff are greatly appreciated.

References

1. Farrar, C.R., and Worden, K. (2007). An introduction to structural health monitoring. *Philosophical Transactions of the Royal Society of London A: Mathematical, Physical and Engineering Sciences*, 365(1851), 303-315.
2. Doebling, S.W., Farrar, C.R., and Prime, M.B. (1998). A summary review of vibration-based damage identification methods. *Shock and Vibration Digest*. 30(2), 91-105.
3. Fan, W., and Qiao, P. (2011). Vibration-based damage identification methods: a review and comparative study. *Structural Health Monitoring*. 10(1), 83-111.
4. Wang, X., Hutchinson, T.C., Hegemeir, G., Gunisetty, S., Kamath, P., and Meacham, B. (2016). Earthquake and post- earthquake fire performance of a mid-rise cold-formed steel framed building - test program and test results: Rapid Release Report (CFS Test Program Report #1). *Structural Systems Research Project. Report No. SSRP-16/07*. University of California, San Diego. La Jolla, CA.
5. Wang, X., Hutchinson, T.C., Hegemeir, G., Gunisetty, S., Kamath, P., and Meacham, B. (2017). Earthquake and post- earthquake fire performance of a mid-rise cold-formed steel framed building - test program and test results: Final Report (CFS Test Program Report #2). *Structural Systems Research Project. Report No. SSRP-16/08*. University of California, San Diego. La Jolla, CA.
6. Hutchinson, T.C., Wang, X., Hegemeir, G., Meacham, B., and Kamath, P. (2018). Earthquake and Post-Earthquake Fire Testing of a Mid-Rise Cold-Formed Steel Framed Building. *Proceedings of the 11th National Conference in Earthquake Engineering,* Earthquake Engineering Research Institute, Los Angeles, CA.
7. AISI (American Iron and Steel Institute) (2007). *North American standard for cold-formed steel farming—Lateral design*. AISI S213, Washington, DC.
8. AISI (American Iron and Steel Institute) (2012). *North American specification for the design of cold-formed steel structural members.* AISI S100, Washington DC.
9. ASCE (American Society of Civil Engineers) (2010). *Minimum Design Loads for Buildings and*

Other Structures. ASCE 7, Reston, VA.

10. Van Overschee, P. and De Moor, B. (1996). *Subspace Identification for Linear systems: Theory, Implementation, Applications.* Kluwer academic publishers, Boston, MA.
11. Moaveni, B., He, X., Conte, J.P., Restrepo, J.I., and Panagiotou, M. (2010). System identification study of a 7-story full-scale building slice tested on the UCSD-NEES shake table. *ASCE Journal of Structural Engineering*, 137(6), 705-717.
12. Belleri, A., Moaveni, B., and Restrepo, J.I. (2014). Damage assessment through structural identification of a three-story large-scale precast concrete structure. *Earthquake Engineering & Structural Dynamics*, 43(1), 61-76.
13. Astroza, R., Ebrahimian, H., Conte, J.P., Restrepo, J.I., and Hutchinson, T.C. (2016). System identification of a full- scale five- story reinforced concrete building tested on the NEES-UCSD shake table. *Structural Control and Health Monitoring*, 23(3), 535-559.
14. Heylen, W., Lammens, S., and Sas, P. (1995). *Modal analysis testing and theory.* PMA-KU Leuven, Belgium.
15. Allemang, R.J., and Brown, D. L. (1982). A correlation coefficient for modal vector analysis. *Proc., 1st International Modal Analysis Conference,* Orlando, FL.